THE JOURNAL OF PHYSICAL CHEMISTRY A

ARTICLE

pubs.acs.org/JPCA

Mapping Molecular Conformations with Multiple-Mode Two-Dimensional Infrared Spectroscopy

Hongtao Bian,[†] Jiebo Li,[†] Xiewen Wen,[†] Zhigang Sun,[‡] Jian Song,[‡] Wei Zhuang,[‡] and Junrong Zheng*[,†]

[†]Department of Chemistry, Rice University, Houston, Texas 77005, United States

[‡]State Key Laboratory of Molecular Reaction Dynamics, Dalian Institute of Chemical Physics, Chinese Academy of Sciences, Dalian 116023, Liaoning, People's Republic of China

Supporting Information

ABSTRACT: The multiple-mode two-dimensional infrared (2D-IR) spectrum in a broad frequency range from 1000 to 3200 cm^{-1} of a 1-cyanovinyl acetate solution in CCl_4 is reported. By analyzing its relative orientations of the transition dipole moments of normal modes that cover vibrations of all chemical bonds, the three-dimensional molecular conformations and their population distributions of 1-cyanovinyl acetate are obtained, with the aid of quantum chemistry calculations that translate the experimental transition dipole moment cross angles into the cross angles among chemical bonds.

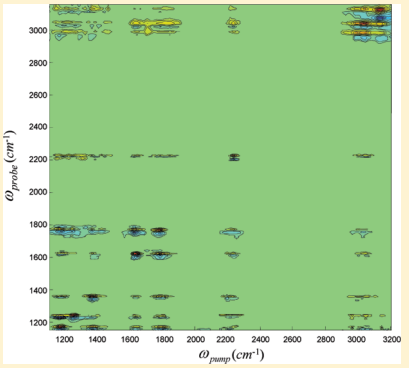

1. INTRODUCTION

Fast molecular conformational fluctuations in the condensed phases play critical roles in many important chemical and biological activities,[1,2] for example, chemical reactions, protein foldings, and molecular recognitions. Tremendous efforts have been devoted to develop tools to monitor the real-time three-dimensional molecular conformations in these biological processes. Among many powerful techniques developed, the multiple-dimensional nuclear magnetic resonance (NMR) methods are the most successful for this purpose so far.[3] However, the low intrinsic temporal resolution (the pulses are longer than 10^{-6} seconds) of NMR determines that structures of faster fluctuations from the methods are only the long-time average.

The infrared (IR) spectroscopic techniques that describe the nuclear motions (bond vibrations) have a sufficient high temporal resolution ($\sim 10^{-14}$ seconds).[4] However, most IR methods are linear, only providing information about the frequencies of molecular vibrations. In general, molecular vibrational frequencies in condensed phases are sensitive not only to the molecular bond connectivity but also to the solute/solvent interactions.[4−6] In addition, the conformational changes of a molecule may have very little effect on the frequencies of some highly localized modes. Accidental degeneracies can also cause extremely difficult peak assignments for an IR spectrum.[7] All of these limiting factors impose great difficulties for linear IR methods to determine three-dimensional molecular conformations.

The expansion of 1D NMR into 2D NMR revolutionarily enlarges its capability of resolving molecular structures.[3] Inspired by the success, scientists have devoted to explore whether the miracle can be reproduced in the optical region.[8−12] 2D-IR was developed more or less under such a scenario in the past decade.[13−22] In principle, it is possible to determine the three-dimensional molecular conformations by 2D-IR methods: (1) the relative orientations of the chemical bonds of a molecule can be determined by the experimentally determined relative orientations of the transition dipole moments of vibrations; (2) the relative chemical bond distances can be obtained from the experimentally determined vibrational couplings or anharmonicities. Certainly, to realize this ultimate goal, in addition to the advance of experimental techniques, theories and databases to connect the experimental observables and molecular structures are also indispensable. In practice, because of technical difficulties, the goal seems to be fairly remote. For example, the couplings among modes which are separated by two or more bonds, or among modes of wide frequency separations and with weak transition dipole moments, are too weak to be detected by most current 2D-IR methods.

In order to obtain the complete three-dimensional conformations of a molecule, vibrations covering all chemical bonds of which the frequencies reside in a wide mid-IR range must be simultaneously investigated. Information from one or a few modes can only provide partial knowledge about the structure

Received: January 18, 2011
Revised: March 10, 2011
Published: March 25, 2011

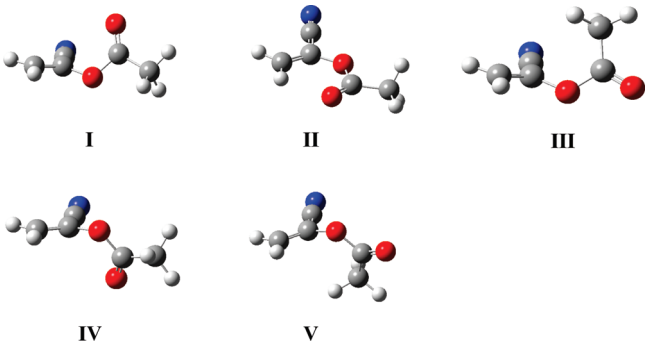

Figure 1. B3LYP/6-311++G(d,p) optimized structures of the 1-cyanovinyl acetate in the CCl_4 phase using the CPCM model.

of the molecule. One of the main practical obstacles in mapping three-dimensional molecular conformations with most current 2D-IR methods is the lack of sufficient pump power with tunable frequencies covering the whole mid-IR range. We recently designed a multiple-mode 2D-IR method which always has more than enough power covering the frequency range from 4000 to 900 cm^{-1} (with two recent upgrades, it now covers the whole mid-IR range).[23,24] The setup technically allows us to explore the possibility of determining the three-dimensional molecular conformations in experiments.

In this work, we report our first attempt in this direction. The molecule selected to study is 1-cyanovinyl acetate. Its structures and conformations are displayed in Figure 1. This molecule has several advantages to serve as the model system for the study; (1) it is small enough that the current ab initio calculations can relatively precisely predict many of its molecular properties; (2) it has several possible conformations; (3) it has many typical vibrational groups, for example, C═C−H, C−C−H, C≡N, C═C, C═O, and C−O; (4) these vibrational groups cover all of the molecular space, and therefore, it is possible that the three-dimensional conformations of this molecule can be obtained by investigating the vibrations of these groups; and (5) these vibrational groups covers a big vibrational frequency range (>2000 cm^{-1}) and a big vibrational spatial separation (more than three chemical bonds), which allows us to explore the sensitivity and potential of our approach.

2. EXPERIMENTS

The optical setup was described previously.[23] Briefly, a picosecond amplifier and a femtosecond amplifier are synchronized with the same seed pulse. The picosecond amplifier pumps an OPA to produce ∼0.8 ps (vary from 0.7 to 0.9 ps in different frequencies) mid-IR pulses with a bandwidth of ∼21 cm^{-1} in a tunable frequency range from 400 to 4000 cm^{-1} with energy 1−40 μJ/pulse (1−10 μJ/pulse for 400−900 cm^{-1} and >10 μJ/pulse for higher frequencies) at 1 kHz. The femtosecond amplifier pumps another OPA to produce ∼140 fs mid-IR pulses with a bandwidth of ∼200 cm^{-1} in a tunable frequency range from 400 to 4000 cm^{-1} with energy 10−40 μJ/pulse at 1 kHz. In 2D-IR and pump/probe experiments, the picosecond IR pulse is the pump beam (pump power is adjusted based on need, and the interaction spot varies from 100 to 500 μm). The femtosecond IR pulse is the probe beam, which is frequency resolved by a spectrograph (resolution is 1−3 cm^{-1}, dependent on the frequency), yielding the probe axis of a 2D-IR spectrum. The temporal shapes of the IR pulses are mostly Gaussian (see Figure S1 in Supporting Information, SI). Scanning the pump frequency yields the other axis of the spectrum. Two polarizers are added into the probe beam path to selectively measure the parallel or perpendicular polarized signal relative to the pump beam. Vibrational lifetimes are obtained from the rotation-free 1−2 transition signal $P_{life} = P_{\parallel} + 2 \times P_{\perp}$, where $P_{\parallel}$ and $P_{\perp}$ are parallel and perpendicular data, respectively. Rotational relaxation times are acquired from $\tau = (P_{\parallel} - P_{\perp})/(P_{\parallel} + 2 \times P_{\perp})$. The whole setup including the frequency tuning is computer-controlled. The alignment and synchronization of the experiments are very straightforward because of the two-beam configuration and the high pump power (a visible guide beam is not required because a liquid crystal card is good enough to see where the IR beams are). These features make it very user-friendly.

1-Cyanovinyl acetate was purchased from Aldrich and used as received. Samples for the FTIR and 2D-IR measurements were contained in sample cells composed of two CaF_2 windows separated by a Teflon spacer. The thickness of the spacer was adjusted based on the optical densities of different modes from 2.5 to 250 μm. 1-Cyanovinyl acetate was dissolved into CCl_4, where its concentration was controlled to maintain an optical density (OD) of ∼0.5 in the measured probe frequency. The experimental optical path and apparatus after the generation of mid-IR pulses was purged with CO_2- and H_2O-free clean air. All of the measurements were carried out at room temperature (22 °C).

The structures were determined with density functional theory (DFT) calculations. The DFT calculations were carried out using Gaussian 09. The level and basis set used were Becke's 3-parameter hybrid functional combined with the Lee−Yang−Parr correction functional, abbreviated as B3LYP, and 6-311++G(d,p).

3. RESULTS AND DISCUSSION

3.1. Possible Conformations of 1-Cyanovinyl Acetate. Our DFT calculation results show that there are five possible conformers for 1-cyanovinyl acetate in gas and in CCl_4. The optimized structures are listed in Figure 1. The five conformers are the isomerization results rotating around the two C−O single bonds. In all conformers, the C═C and C≡N bonds are always in the same plane. Conformers I and IV are mirror symmetric to each other. They are the most stable conformations. Conformers III and V have much higher energy than the others (∼5 kcal/mol). On the basis of the calculated energy values, they are negligible conformers at room temperature. Table 1 gives the calculated energies, bond lengths, and key dihedral angles of the 1-cyanovinyl acetate molecule.

3.2. Linear FTIR and 2D-IR Spectra. The FTIR spectrum of 1-cyanovinyl acetate in CCl_4 is shown in Figure 2. The peak assignments, C═O (1788 cm^{-1}), C═C (1639 cm^{-1}), C≡N (2236 cm^{-1}), C−H (2942, 2995, 3047, and 3135 cm^{-1}), C−O stretch (1180 and 1248 cm^{-1}), and C−H bending (1372 and 1430 cm^{-1}), are marked in Figure 2.

Different from the linear FTIR spectrum in Figure 2, where only the 0−1 transition frequencies of vibrational modes of the molecule are acquired, the multiple-mode 2D-IR spectrum in Figure 3 provides much more molecular information. Both 0−1 and 1−2 vibrational transition frequencies are obtained from the positions of the diagonal red and blue peaks. The vibrational coupling anharmonicities among vibrational modes are manifested by the positions of the off-diagonal peak pairs. The relative orientations of the vibrations are obtained from the polarization-selective

Table 1. Calculated Energies, Bond Lengths, and Dihedral Angles (degrees) for the Five Optimized Conformers of 1-Cyanovinyl Acetate Calculated at the B3LYP 6-311++G(d,p) Level in Gas and CCl_4 using SCRF-CPCM

		conformers				
		I	II	III	IV	V
in Gas	ΔE/kcal mol^{-1}	0.00	0.23	5.09	0.00	5.09
	(C−C−O−C)/deg.	66	−180	69	−66	−69
	(C−O−C═O)/deg.	5	0	−180	−5	180
	bond lengths/Å	C═C (1.33), C≡N (1.16), C−O(1.39), C═O(1.21), C−C(C≡N) (1.44), C−C (CH_3) (1.50), C−H (CH_2) (1.08), C−H (CH_3) (1.09)				
in CCl_4	ΔE/kcal mol^{-1}	0.00	0.97	4.68	0.00	4.68
	(C−C−O−C)/deg.	66	−180	75	−66	−75
	(C−O−C═O)/deg.	3	0	−180	−3	180
	bond lengths/Å	C═C (1.33), C≡N (1.16), C−O (1.39), C═O (1.21), C−C(C≡N) (1.44), C−C (CH_3) (1.50), C−H (CH_2) (1.08), C−H (CH_3) (1.09)				

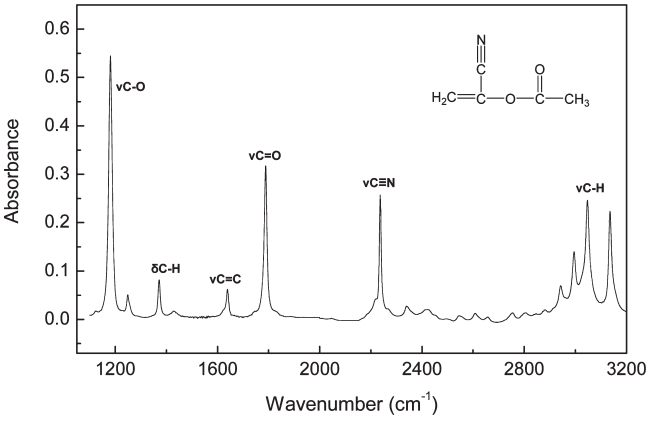

Figure 2. FTIR spectrum of 1-cyanovinyl acetate in CCl_4. (Inset) Molecular formula of 1-cyanovinyl acetate.

measurements of the off-diagonal peak intensities. The detailed analysis is given in the next section.

3.3. Cross Angles among Vibrations. When two vibrational modes are anharmonically coupled with each other and the coupling is sufficiently strong (e.g., >1 cm^{-1}), off-diagonal peak pairs will appear in the 2D-IR spectra, as demonstrated in Figure 4a (an enlarged part of Figure 3) for the C═C and C═O modes of 1-cyanovinyl acetate. The amplitudes of the off-diagonal peaks are dependent on the polarizations of the exciting and probing beams,[13,25−27] as shown in Figure 4b. This is because the transition dipole moments of the two coupled modes are aligned to each other with a certain cross angle which is determined by the molecular conformation. If the polarization angle between the exciting and probing beams is the same as the vibrational cross angle, the intensities of the off-diagonal peaks will be maximum. Experimentally, by changing the polarizations of the laser beams, the vibrational cross angles can be straightforwardly determined based on the following two equations. For two coupled modes, the anisotropy R of their combination band peaks is correlated with the angle θ between their transition dipole moments in the form of

$$R = \frac{3\cos^2\theta - 1}{5} \qquad (1)$$

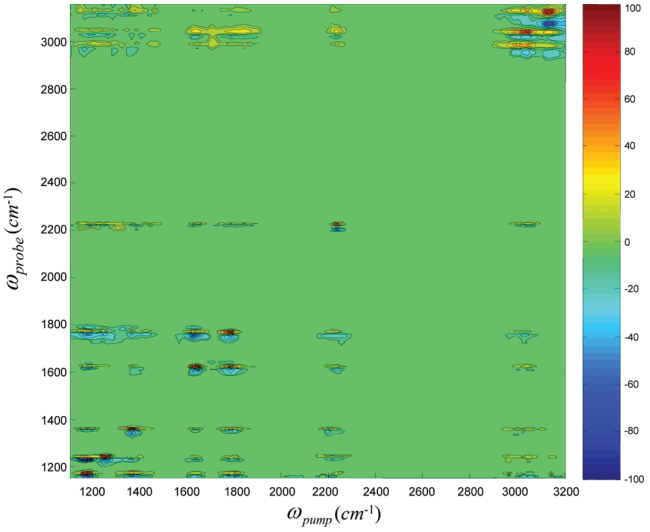

Figure 3. 2D-IR spectrum of 1-cyanovinyl acetate at a waiting time of 0.2 ps. The relative intensities of peaks are adjusted to be comparable. Detailed factors are provided in the SI. Each contour represents a 10% amplitude change.

Equation 1 can also be expressed by the following form

$$\frac{I_\perp}{I_\parallel} = \frac{2 - \cos^2\theta}{1 + 2\cos^2\theta} \qquad (2)$$

where $I_\parallel$ and $I_\perp$ are peak intensities from experiments with parallel and perpendicular pump/probe polarizations, respectively.

From the experimental measurements (Figure 4b), the averaged $I_\perp/I_\parallel$ intensity ratio is determined to be 1.4 ± 0.1. From eq 2, the angle between the transition dipole moments of C═C and C═O is determined to be 66 ± 3°. The intensities were obtained by fitting the peaks with Gaussian to remove the effect of overlapping.

To verify the value that we obtained, the other off-diagonal blue peak (1639, 1776 cm^{-1}) was also measured. (For all of the angle measurements, we always use the off-diagonal blue peaks. Red peaks are also measured. Data and discussion about the difference between these two types of peaks and possible reasons for the difference are provided in the SI.) The averaged $I_\perp/I_\parallel$ intensity ratio is determined to be 1.3 ± 0.1. The angle

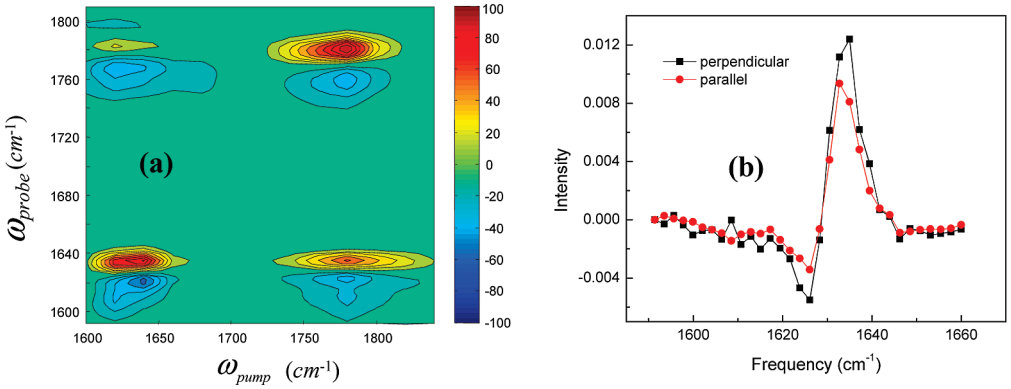

Figure 4. (a) Enlarged 2D-IR spectrum of 1-cyanovinyl acetate at a waiting time of 0.2 ps in the C═C and C═O frequency range. The detection polarization is parallel with the pump. (b) Off-diagonal pump−probe spectra with the probe in the C═C region and the pump at 1784 cm^{-1} (C═O), measured at the 0.2 ps delay. Both the parallel (top) and perpendicular (bottom) data are shown. Each contour represents a 10% amplitude change.

Table 2. Transition Dipole Moment Angle between Coupled Vibrational Modes of the 1-Cyanovinyl Acetate Molecule Determined from the Anisotropy Measurement[a]

pair number	coupled modes	relative angle (degrees)	pair number	coupled modes	relative angle (degrees)
1	C═C/C═O	64 ± 3	10	C═O/CH_2(as)	58 ± 3
2	C═C/C≡N	43 ± 3	11	C═O/CH_3(as)	55 ± 3
3	C═C/C−O(as)	37 ± 5	12	C≡N/C−O(as)	69 ± 3
4	C═C/CH_2(as)	37 ± 5	13	C≡N/CH_2(as)	47 ± 5
5	C═C/CH_2(ss)	43 ± 5	14	C≡N/CH_2(ss)	37 ± 5
6	C═C/CH_3(as)	37 ± 5	15	C≡N/CH_3(as)	43 ± 5
7	C═O/C≡N	58 ± 3	16	C−O(as)/CH_2(as)	55 ± 3
8	C═O/C−O(as)	78 ± 3	17	C−O(as)/CH_2(ss)	51 ± 3
9	C═O/C−O(ss)	47 ± 5			

[a] The anisotropy data were obtained at a waiting time of 0.2 ps. (The uncertainty from molecular rotation is not listed.)

between the transition dipole moments of C═O and C═C is determined to be 64 ± 3°. This value is consistent with the above value.

The transition dipole moment angles of other coupled modes were also obtained using the same procedure. The results are listed in Table 2 (data are shown in SI). In the experiment, because the light polarization is 0−90°, the angles determined are also in this range. The rotational time constant of a 1-cyanovinyl acetate molecule is around 4.0 ps (see SI). In our cross angle calculation procedures, the transition dipole moment angles of all of the coupled modes are determined at a waiting time of 0.1−0.2 ps. In our experiments, the pump pulse is ∼0.8 ps, and the probe pulse is ∼0.14 ps; the overlapping between them causes a temporal uncertainty of about 0.2−0.3 ps. Because the molecular rotation is relatively short, this temporal uncertainty causes an uncertainty of ∼10° in the determined transition dipole moment angle. This uncertainty range is confirmed by measuring the diagonal anisotropy (see Figures S2(b) and S3(b) in SI). The anisotropy decay during this pulse interaction period cannot be recovered by measuring the waiting-time-dependent decay curve and simply extrapolating back to time zero because many of these modes have very apparent relaxation-induced signal changes. Great care must be taken to do the time delay correction. Methods to recover the initial decay will be investigated in the future.

3.4. Averaged Molecular Conformation. One major difficulty in converting 2D-IR measurements into molecular structures is that the vector direction of the transition dipole moment of a vibrational mode is mostly different from that of the chemical bond which is mainly responsible for the vibration. Even for a highly localized mode, its direction is still slightly different from the bond orientation. Therefore, the vibrational cross angles presented in the above section cannot be immediately translated into the relative orientations of the chemical bonds. However, on one hand, corresponding to a well-defined molecular conformation, there is one and only one set of spatially well-defined vibrations because the vibrational motions are purely determined by the bond orientations. On the other hand, corresponding to one set of spatially well-defined vibrations, there is one and only one set of chemical bond orientations of the molecule. In other words, the relation between the orientations of bonds and vibrations is one-to-one. Therefore, the translation of the vibrational cross angles into relative bond orientations is more like converting data from one coordinate system to another, though the conversion of the coordinate systems (vibrational coordinates into atomic coordinates) is not very straightforward. The commercial ab initio calculation program Gaussian has such a function to translate atomic coordinates into vibrational coordinates. With the aid of such a function from the ab initio calculations, in principle, the molecular conformation can be revealed from the

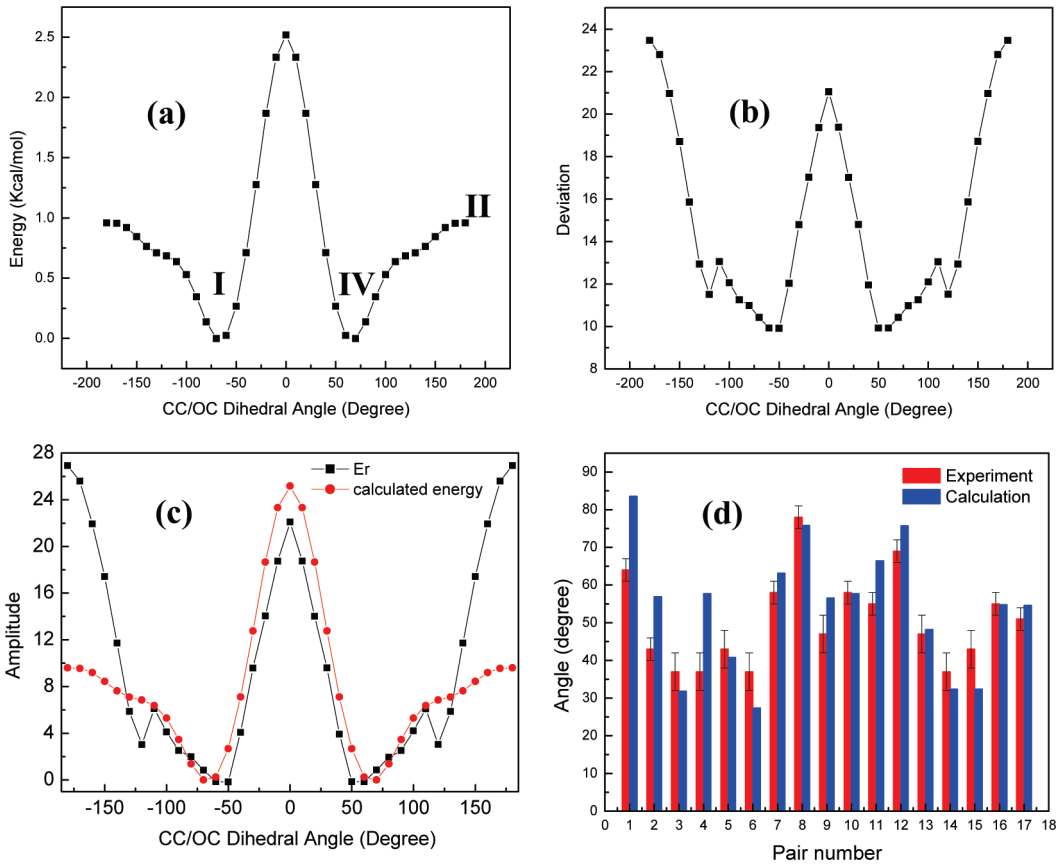

Figure 5. (a) Calculated potential energy surface (PES) of the 1-cyanovinyl acetate in CCl_4. (b) Deviation Er vs the CC/OC dihedral angle. (c) Rescaled PES and Er. (d) Calculated and experimental average vibrational cross angles of the 17 coupling pairs.

2D-IR measurements. In the following, the procedure to translate the experimental data into molecular conformation is described.

Ideally, it would be most straightforward if the atoms could be assembled into the right molecular conformations by calculations based on the experimentally determined vibrational angles. However, the currently available program in Gaussian optimizes the molecular conformation first and then calculates all properties including the vibrational angles based on the optimized structure. Such a calculating procedure determines that the translation of the experimental observables into the molecular conformations is more like a fitting procedure; instead of using the energy minimum (default) as the structural criterion, the experimental vibrational cross angles will serve as the criterion to determine which calculated conformations are closest to that experimentally observed. The general calculation procedure would be extremely time-consuming and would include calculating the vibrational angles of each possible conformation of which the number can be infinite and comparing them to the experimental data until the closest values are found. For 1-cyanovinyl acetate, because of its structural constraints, the possible conformations are not that many. The major degree of freedom to generate different conformations is the rotation around the two C−O single bonds. We therefore optimized the molecular conformations at different C−C/C−O (of the acid group) dihedral angles and calculated their minimum energy and the vibrational cross angles of the 17 pairs of normal modes experimentally investigated. The energy minima and the deviation Er's between the calculated and experimental vibrational cross angles are shown in Figure 5. Er is expressed in the following equation

$$\mathrm{Er} = \frac{\sum_{i=1}^{m} |A_i^{\mathrm{C}} - A_i^{\mathrm{E}}|}{m} \qquad (3)$$

where A_i^{C} is the calculated vibrational cross angles of ith pair of normal modes. A_i^{E} is the experimental value listed in Table 2, and m is the number of the coupling pairs, which is 17.

As shown in Figure 5c, it is surprising that calculations based on both the energy minimum and experimental vibrational cross angles criteria give almost the same most probable conformations. At the most probable conformations (almost the energy minima), the calculated vibrational cross angles are about 10° different from the experimental results on average. To more quantitatively compare the calculated and experimental vibrational cross angles, we define another parameter to account for the distribution of conformations, the averaged angle $\overline{A}$ as

$$\overline{A} = \frac{\sum_{i=1}^{n} A_i \cdot \rho_i}{\sum_{i=1}^{n} \rho_i} \qquad \rho_i = \exp\left(\frac{E_i - E_0}{kT}\right) \qquad (4)$$

where E_i is the calculated energy of conformation i, E_0 is the lowest energy, and ρ_i is the Boltzmann distribution. The calculated $\overline{A}$ and experimental vibrational cross angles are plotted in

dx.doi.org/10.1021/jp200516p |J. Phys. Chem. A 2011, 115, 3357–3365

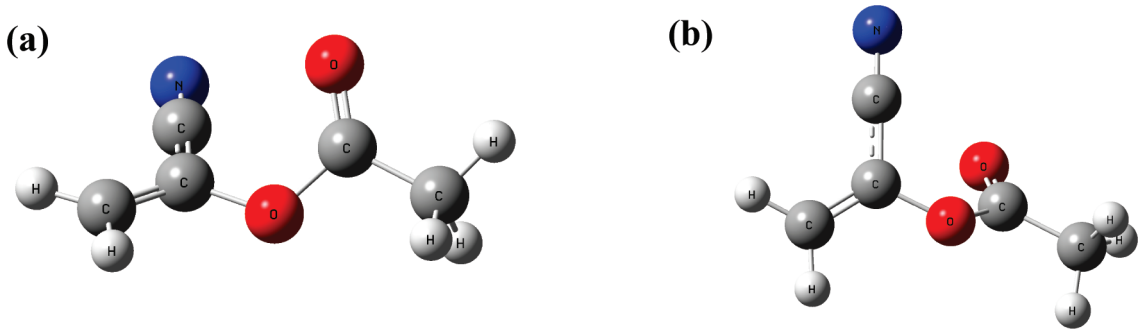

Figure 6. The most probable molecular conformations determined by the experimental vibrational angles. (a) With a C−C/C−O (of the acid group) dihedral angle of ∼50°; (b) mirror symmetric conformation of (a). Within experimental and calculated uncertainties, we consider these two conformations to be identical to I and IV in Figure 1.

Table 3. Computed Diagonal Anharmonicities for Conformers I, II, and III of the 1-Cyanovinyl Acetate with the Normal Modes Frequencies Higher than 1000 cm^{-1} Calculated at the B3LYP 6-311++G(d,p) Level in CCl_4 and Experimental Anharmonicities and Mode Frequencies

			calculated diagonal anharmonicities (cm^{-1})			
normal mode	assignment	experimental frequency (cm^{-1})	conf. I	conf. II	conf. III	experimental value (cm^{-1})
20	C−O as	1180	9.3	12.0	9.0	15
21	C−O ss	1250	2.3	4.6	9.0	13
22	CH_3 bending	1371	17.6	16.0	18.2	15
23	CH_2 scissoring	1371	5.7	10.1	6.2	
24	CH_3 bending	1430	12.8	12.0	−2.1	
25	CH_3 bending	1430	15.5	12.3	13.4	
26	C═C stretch	1639	10.2	7.4	11.6	11
27	C═O stretch	1787	24.3	22.7	26.2	16
28	C≡N stretch	2236	22.8	23.6	22.6	22
29	CH_3 ss	2940	45.1	41.5	45.1	
30	CH_3 as	2995	66.2	63.1	64.2	
31	CH_2 ss	3046	89.3	86.6	119.5	
32	CH_3 as	3046	86.7	106.8	87.7	
33	CH_2 as	3135	65.2	75.8	66.8	44

Figure 5d. For most coupling pairs, the difference between calculated and experimental results is only a few degrees. Within experimental uncertainty (∼10°), the consistency between the calculated and experimental results is surprisingly good.

On the basis of the above analysis, the most probable molecular conformations experimentally determined are two conformations (in Figure 6) with the dihedral angles of C−C and C−O (of the acid group) around 50 and −50°, respectively. However, the energy difference between these two conformations and I and IV in Figure 1 is smaller than 0.1 kcal/mol. Within experimental and calculation uncertainties, we would consider that the experimentally most probable conformations are also the calculated most stable conformations.

3.5. Vibrational (Diagonal) and Coupling (Off-Diagonal) Anharmonicities. Another type of important molecular information from 2D-IR measurements is the vibrational and coupling anharmonicities. In principle, these two types of anharmonicities are also correlated with the molecular conformations and vibrational spatial separations (especially the coupling anharmonicities), though the correlations are much less straightforward than that between the vibrational cross angles and chemical bond angles. In this section, we will explore what structural information can be obtained from the anharmonicity measurements and the ab initio calculations.

Diagonal (vibrational) anharmonicity (Δ_{ii}) was determined as the frequency difference between the 0−1 transition (red peak) and 1−2 transition (blue peak) of the diagonal peak pair in 2D-IR spectra (Figures 3 and 4). The diagonal anharmonicities and their frequencies of each vibrational normal mode of 1-cyanovinyl acetate are listed in Table 3.

Using the second-order vibrational perturbation theory (PT2), the anharmonic and harmonic frequencies of the fundamental transitions and anharmonic overtone transition frequencies for the total $3N - 6$ normal modes of the 1-cyanovinyl acetate were obtained by the ab initio calculations. The diagonal ($3N - 6$) and off-diagonal ($(3N - 6)(3N - 5)/2$) anharmonicities were calculated. The approach to calculate the diagonal and off-diagonal anharmonicities is straightforward and has been adopted by many groups.[28] The calculated diagonal anharmonicities of conformers I, II, and III with the normal-modes frequency higher than 1000 cm^{-1} are also listed in Table 3.

From Table 3, the calculated diagonal anharmonicities (Δ_{ii}) are qualitatively consistent with experimental results. However, for some modes, the calculated conformational dependence of

Table 4. Computed off-Diagonal Anharmonicities for Conformers I, II, and III Calculated at the B3LYP 6-311++G(d,p) Level in CCl_4 and Experimental Determined off-Diagonal Anharmonicities

coupled modes	coupled modes	conf. 1	conf. 2	conf. 3	experimental value (cm^{-1})
26/20	C═C/C−O as	1.465	0.481	1.852	6 ± 1
26/21	C═C/C−O ss	2.138	6.088	8.035	
26/22	C═C/CH_3 bending	−0.558	−0.474	0.544	
26/23	C═C/CH_2 scissoring	−25.391	19.521	34.950	
26/24	C═C/CH_3 bending	−0.828	0.356	−6.385	
26/25	C═C/CH_3 bending	−0.144	−1.149	0.490	
26/27	C═C/C═O	−0.977	−0.256	2.862	6 ± 1
26/28	C═C/C≡N	1.037	1.098	2.536	6 ± 1
26/29	C═C/CH_3 ss	−0.729	−0.688	0.528	
26/30	C═C/CH_3 as	0.822	−2.127	0.499	11 ± 1
26/31	C═C/CH_2 ss	−16.835	−1.200	44.253	11 ± 1
26/32	C═C/CH_3 as	−0.735	28.345	0.470	11 ± 1
26/33	C═C/CH_2 as	−2.634	2.799	−1.007	10 ± 1
27/20	C═O/C−O as	3.346	−1.964	1.001	8 ± 1
27/21	C═O/C−O ss	1.868	−0.568	5.057	8 ± 1
27/22	C═O/CH_3 bending	0.496	0.303	2.920	
27/23	C═O/CH_2 scissoring	−0.391	3.137	1.953	
27/24	C═O/CH_3 bending	1.417	−0.019	−4.143	
27/25	C═O/CH_3 bending	1.407	0.255	2.776	
27/28	C═O/C≡N	0.033	−0.170	1.761	
27/29	C═O/CH_3 ss	1.307	1.298	3.239	7 ± 1
27/30	C═O/CH_3 as	2.767	−0.133	3.327	8 ± 1
27/31	C═O/CH_2 ss	−28.133	0.228	32.527	9 ± 1
27/32	C═O/CH_3 as	0.622	14.472	2.255	8 ± 1
27/33	C═O/CH_2 as	−0.190	0.787	1.869	8 ± 1
28/20	C≡N/C−O as	1.373	0.365	0.725	6 ± 1
28/21	C≡N/C−O ss	0.883	0.863	3.753	10 ± 1
28/22	C≡N/CH_3 bending	0.037	−0.088	0.056	
28/23	C≡N/CH_2 scissoring	−0.203	2.597	0.200	
28/24	C≡N/CH_3 bending	0.118	−0.022	−7.058	
28/25	C≡N/CH_3 bending	0.632	−0.372	0.122	
28/29	C≡N/CH_3 ss	−0.035	−0.046	0.021	11 ± 1
28/30	C≡N/CH_3 as	1.555	−1.177	0.036	11 ± 1
28/31	C≡N/CH_2 ss	−28.222	−0.447	30.687	13 ± 1
28/32	C≡N/CH_3 as	−0.032	14.113	0.052	
28/33	C≡N/CH_2 as	−0.049	0.174	−0.011	12 ± 1

the diagonal anharmonicities is smaller than the fluctuations caused by the selection of different basis sets for calculations (see SI). In addition, the difference between experimentally determined and calculated anharmonicities is larger than those calculated between different conformations. This is probably because of the nature of the calculations. Because the vibrational frequencies are at the order of a few thousand cm^{-1} while the vibrational anharmonicities are only tens of cm^{-1}, it is possible that the perturbation approach used in the calculations will introduce uncertainties of 1−2% of the vibrational frequencies. This issue will be further addressed in our future work.

Off-diagonal anharmonicities were also calculated with a similar procedure. The calculated and experimental data are listed in Table 4. Compared to the diagonal anharmonicities calculations, the computed off-diagonal anharmonicities are obviously not consistent with the experimental data. As mentioned above, the calculations can have uncertainties of tens of cm^{-1}, while the coupling anharmonicities are usually only a few cm^{-1}. It is not surprising that the calculated values are off from those experimentally observed.

Similar to eq 3, we define another criterion which is the difference between the calculated and experimentally determined diagonal and off-diagonal anharmonicity values to search for the most probable molecular conformations. Results are shown in Figure 7. Different from the vibrational angle search in Figure 5, no clear correlation between molecular conformations and anharmonicities is found from Figure 7. From these observations, it seems that without further theoretical developments, it is difficult to predict molecular conformations based on vibrational anharmonicities (at least for the molecule studied here). For ultimately utilizing the vibrational anharmonicitiy information to help determine molecular conformations, we believe that in addition to the advances of theory, the accumulation of a database of correlations among well-defined chemical bond distances and

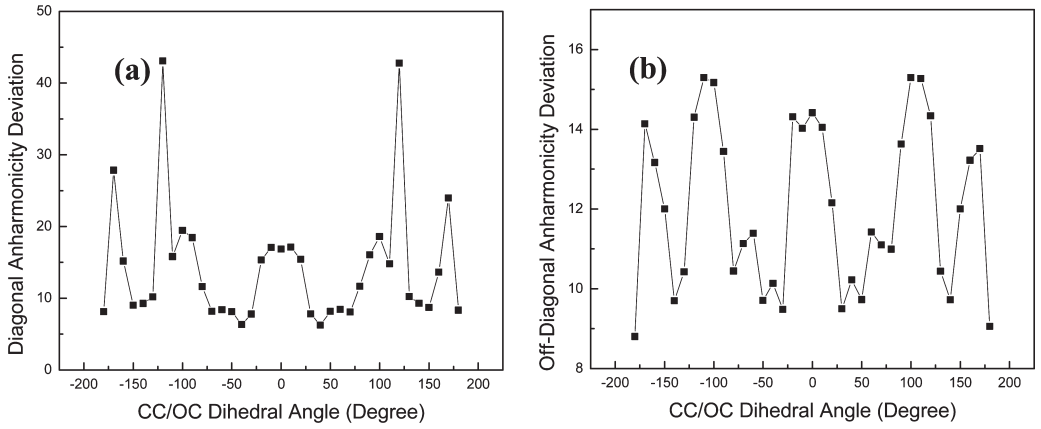

Figure 7. (a) Deviation between the calculated and the experimental diagonal anharmonicity values versus the CC/OC dihedral angle. (b) Deviation between the calculated and the experimental off-diagonal anharmonicity values versus the CC/OC dihedral angle.

orientations and the vibrational anharmonicities and couplings is also very important, which will be pursued in the near future.

4. CONCLUSION

In this report, the multiple-mode two-dimensional infrared (2D-IR) measurements in a broad frequency range from 1000 to 3200 cm^{-1} of a 1-cyanovinyl acetate solution in CCl_4 are reported. By analyzing the relative orientations of the transition dipole moments of normal modes which cover the molecular space of all chemical bonds, the three-dimensional molecular conformations and their population distributions of 1-cyanovinyl acetate are obtained, with the aid of quantum chemistry calculations which translate the experimental transition dipole moment cross angles into the cross angles among chemical bonds. Within experimental and calculated uncertainties, the experimentally determined most probable conformations are identical to the calculated most stable conformations. The molecule studied here is relatively small and therefore has a relatively fast molecular rotational time constant (~4 ps), which causes a relatively big uncertainty (~10°) in the experimentally determined vibrational angles. For bigger molecules, their rotations are slower, and therefore, the vibrational angle uncertainty will be smaller. Their conformations will be more precisely determined by this method. Our experiments and calculations also show that another piece of important molecular information from 2D-IR measurements, vibrational anharmonicities and couplings, is not adequate to help identify molecular conformations for the chemical studied. Theoretical advances and experimental database accumulation are suggested.

Another point that we want to emphasize here is that the design of our multiple-mode 2D-IR setup (full automated control over frequency and delay tuning and data acquisition) is very user-friendly. An undergraduate student can easily operate it after 1 or 2 days of training. It is not more difficult than operating a NMR machine. We believe that this will be very important for the technique to gain more applications in different fields and be operated by researchers who are not professional spectroscopists.

■ ASSOCIATED CONTENT

Supporting Information. Supporting figures and data about the pulse temporal shapes, diagonal anisotropies, and off-diagonal raw data. This material is available free of charge via the Internet at http://pubs.acs.org.

■ AUTHOR INFORMATION

Corresponding Author
*E-mail: junrong@rice.edu.

■ ACKNOWLEDGMENT

This work was supported by Rice University and the Welch foundation. W.Z. thanks DICP for the 100 Talents Support Grant and NSFC for the 2010 QingNian Grant.

■ REFERENCES

(1) DeFlores, L. P.; Ganim, Z.; Nicodemus, R. A.; Tokmakoff, A. *J. Am. Chem. Soc.* **2009**, *131*, 3385.
(2) Finkelstein, I. J.; Zheng, J. R.; Ishikawa, H.; Kim, S.; Kwak, K.; Fayer, M. D. *Phys. Chem. Chem. Phys.* **2007**, *9*, 1533.
(3) Ernst, R. R.; Bodenhausen, G.; Wokaun, A. *Nuclear Magnetic Resonance in One and Two Dimensions*; Oxford University Press: Oxford, U.K., 1987.
(4) Wilson, E. B., Jr.; Decius, J. C.; Cross, P. C. *Molecular Vibrations: The Theory of Infrared and Raman Vibrational Spectra*; McGraw-Hill: New York, 1955.
(5) Surewicz, W. K.; Mantsch, H. H. Infrared Absorption Methods for Examining Protein Structure. In *Spectroscopic Methods for Determining Protein Structure in Solution*; Havel, H. A., Ed.; VCH Publishers, Inc.: New York, 1996; p 135.
(6) Berg, M. A. Vibrational Dephasing in Liquids: Raman Echo and Raman Free-Induction Decay Studies. In *Ultrafast Infrared and Raman Spectroscopy*; Fayer, M. D., Ed.; Marcel Dekker: New York; In press.
(7) Zheng, J.; Kwak, K.; Steinel, T.; Asbury, J. B.; Chen, X.; Xie, J.; Fayer, M. D. *J. Chem. Phys.* **2005**, *123*, 164301.
(8) Zhao, W.; Wright, J. C. *Phys. Rev. Lett.* **2000**, *84*, 1411.
(9) Hybl, J. D.; Ferro, A. A.; Jonas, D. M. *J. Chem. Phys.* **2001**, *115*, 6606.
(10) Hamm, P.; Lim, M.; Degrado, W. F.; Hochstrasser, R. M. *J. Chem. Phys.* **1907**, *2000*, 112.
(11) Asplund, M. C.; Lim, M.; Hochstrasser, R. M. *Chem. Phys. Lett.* **2000**, *323*, 269.
(12) Brixner, T.; Stenger, J.; Vaswani, H. M.; Cho, M.; Blankenship, R. E.; Fleming, G. R. *Nature* **2005**, *434*, 625.
(13) Khalil, M.; Demirdoven, N.; Tokmakoff, A. *J. Phys. Chem. A* **2003**, *107*, 5258.
(14) Bredenbeck, J.; Helbing, J.; Hamm, P. *J. Am. Chem. Soc.* **2004**, *126*, 990.
(15) Shim, S. H.; Strasfeld, D. B.; Ling, Y. L.; Zanni, M. T. *Proc. Natl. Acad. Sci. U.S.A.* **2007**, *104*, 14197.

(16) Baiz, C. R.; Nee, M. J.; McCanne, R.; Kubarych, K. J. *Opt. Lett.* **2008**, *33*, 2533.
(17) Rubtsov, I. V.; Kumar, K.; Hochstrasser, R. M. *Chem. Phys. Lett.* **2005**, *402*, 439.
(18) Maekawa, H.; Formaggio, F.; Toniolo, C.; Ge, N. H. *J. Am. Chem. Soc.* **2008**, *130*, 6556.
(19) Cowan, M. L.; Bruner, B. D.; Huse, N.; Dwyer, J. R.; Chugh, B.; Nibbering, E. T. J.; Elsaesser, T.; Miller, R. J. D. *Nature* **2005**, *434*, 199.
(20) Zheng, J.; Kwak, K.; Asbury, J. B.; Chen, X.; Piletic, I.; Fayer, M. D. *Science* **2005**, *309*, 1338.
(21) Zheng, J.; Kwac, K.; Xie, J.; Fayer, M. D. *Science* **2006**, *313*, 1951.
(22) Bredenbeck, J.; Ghosh, A.; Smits, M.; Bonn, M. *J. Am. Chem. Soc.* **2008**, *130*, 2152.
(23) Bian, H.; Li, J.; Wen, X.; Zheng, J. R. *J. Chem. Phys.* **2010**, *132*, 184505.
(24) Bian, H. T.; Wen, X. W.; Li, J. B.; Zheng, J. R. *J. Chem. Phys.* **2010**, *133*, 034505.
(25) Woutersen, S.; Hamm, P. *J. Phys. Chem. B* **2000**, *104*, 11316.
(26) Zanni, M. T.; Gnanakaran, S.; Stenger, J.; Hochstrasser, R. M. *J. Phys. Chem. B* **2001**, *105*, 6520.
(27) Hahn, S.; Lee, H.; Cho, M. *J. Chem. Phys.* **1849**, *2004*, 121.
(28) Wang, J. P. *J. Phys. Chem. B* **2008**, *112*, 4790.

Mapping Molecular Structure with Multiple-Mode Two-Dimensional Infrared Spectroscopy

Supporting materials

Table S1. Scaling factors for the broad band 2D IR spectrum of 1-cyanovinyl acetate molecule.

Region	Dividing factor	Region	Dividing factor
C=C diagonal	1.0	C-O/C=O	5.0
C=O diagonal	30.0	C-H(b)/C=O	5.0
CN diagonal	1.0	C=C/C=O	1.0
C-H(stretch) diagonal	0.5	CN/C=O	0.5
C-H(bending) diagonal	5.0	C-H(s)/C=O	0.5
C-O diagonal	25.0	C-O/C-H(b)	1.0
C-O(pump)/C-H(probe)	1.0	C=C/C-H(b)	1.0
C-H(b)/C-H(s)	1.0	C=O/C-H(b)	1.0
C=C/C-H(s)	0.5	CN/C-H(b)	0.25
C=O/C-H(s)	0.5	C-H(s)/C-H(b)	0.1
CN/C-H(s)	0.5	C-H(b)/C-O	5.0
C-O/CN	5.0	C=C/C-O	1.0
C-H(b)/CN	5.0	C=O/C-O	1.0
C=C/CN	0.5	CN/C-O	0.25
C=O/CN	0.5	C-H(s)/C-O	0.1
C-H(s)/CN	0.25		

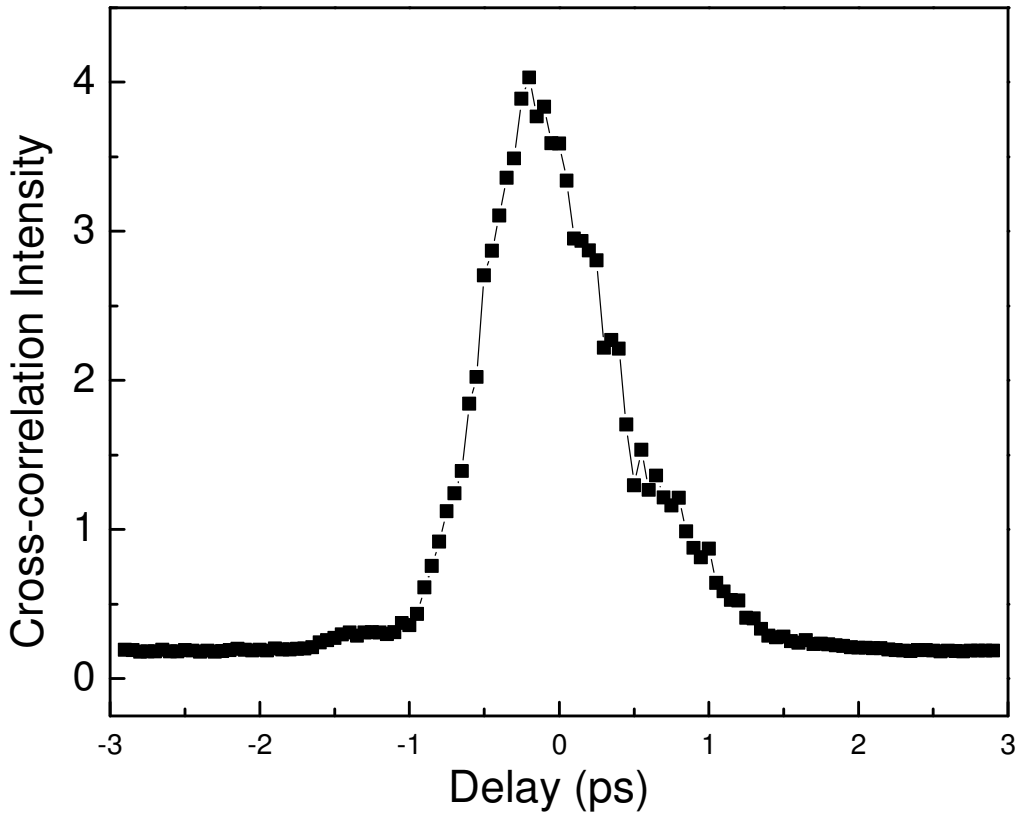

Fig. S1. Cross-correlation of ps and fs OPA outputs at 2065 cm^{-1} with FWHM ~0.9ps. The lineshape is mostly Gaussian. Dependent on the frequency, the FWHM varies from 0.7 ~ 0.9ps.

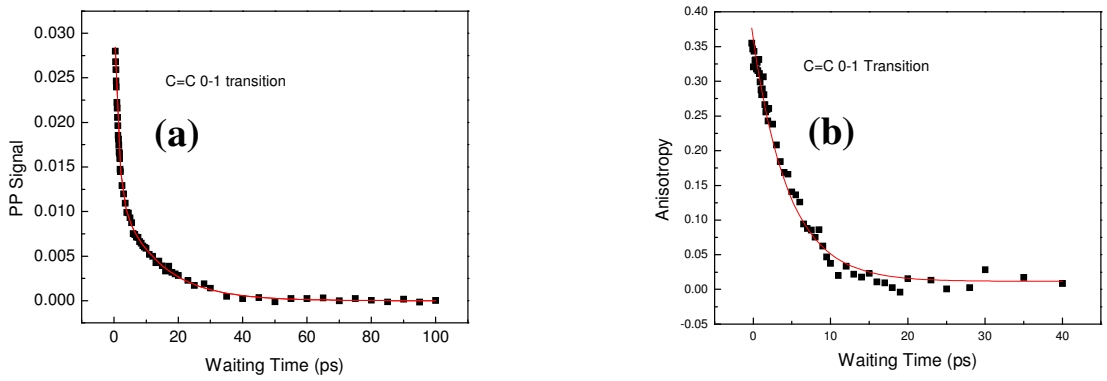

Fig. S2. Pump probe data for the C=C vibrational mode and fitting parameters for the vibrational lifetimes and rotational relaxation time constants. (a) C=C vibrational lifetimes are obtained using two exponential fits which give T_1=1.2ps (65.0%), T_2=13.0ps (35.0%) for the 0-1 transition (1639cm^{-1}); (b) the relaxation time constant for the C=C 0-1 transition is $4.6 \pm 0.6 ps$. The perfect diagonal anisotropy is 0.4. The initial anisotropy here is ~0.37. The 0.03 decay occurs during the pulse interaction duration.

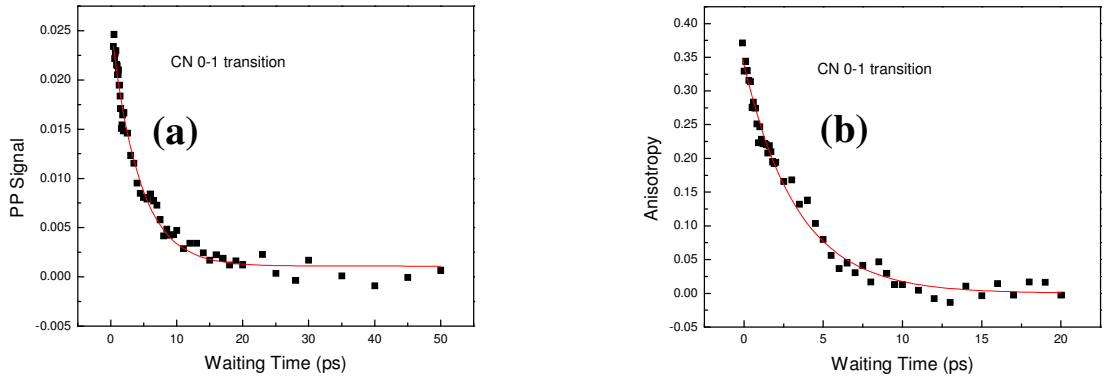

Fig. S3. Pump probe data for the $C \equiv N$ vibrational mode and fitting parameters for the vibrational lifetimes and rotational relaxation time constants. (a) $C \equiv N$ vibrational lifetimes are obtained using one exponential fits which give T_1= 4.2ps for the 0-1 transition (2236cm^{-1}); (b) the relaxation time constant for the $C \equiv N$ 0-1 transition is $3.6 \pm 0.4\,ps$. The perfect diagonal anisotropy is 0.4. The initial anisotropy here is ~0.38. The 0.02 decay occurs during the pulse interaction duration.

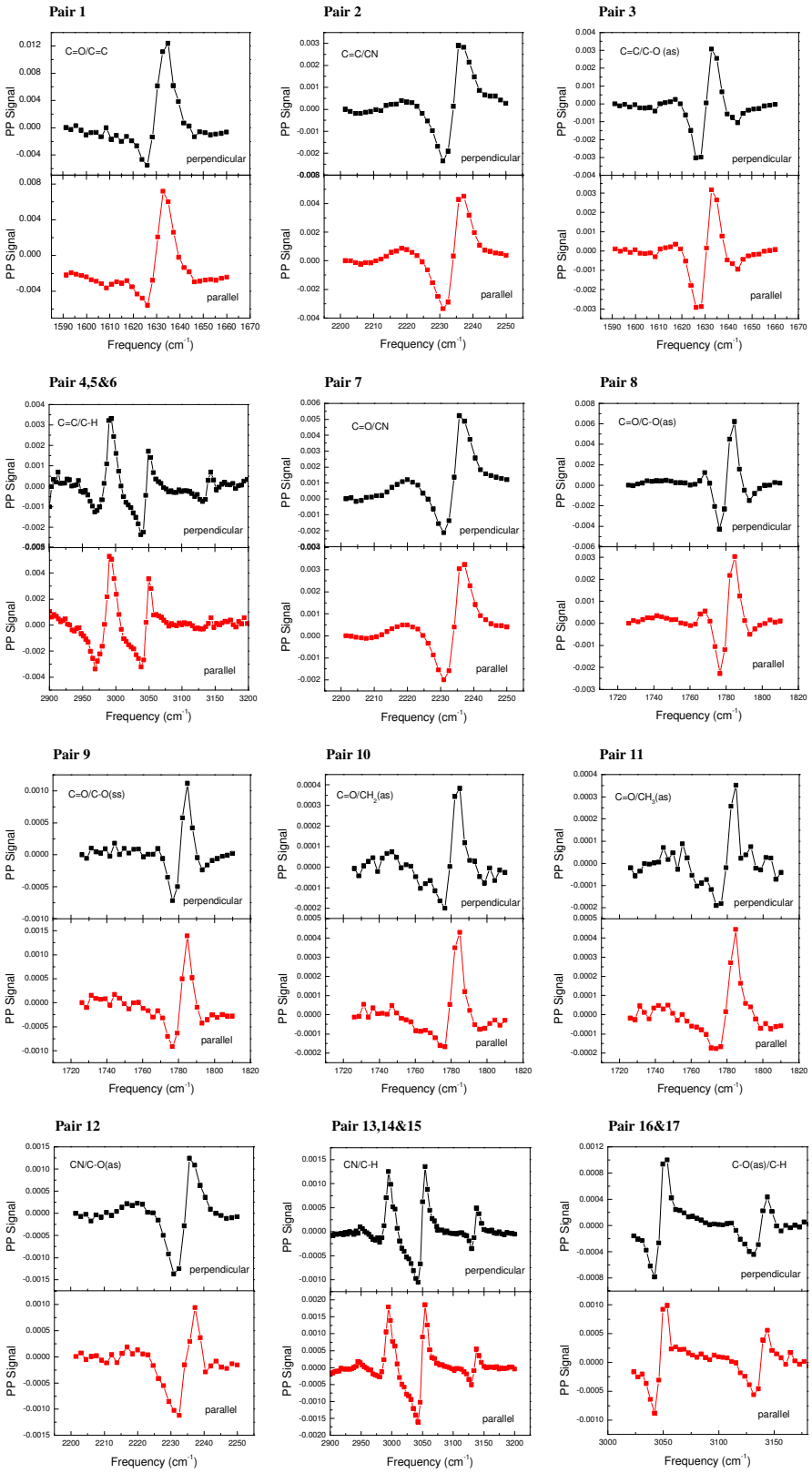

Fig. S4. Pump probe data (parallel and perpendicular) for the 17 pair coupled modes.

Table S2. Computed diagonal anharmonicities for conformer I, II and III of the 1-cyanovinyl acetate with the normal modes frequencies higher than 1000cm^{-1} calculated at B3LYP 6-31+G(d,p) and 6-311++G(d,p) level in CCl_4 phase and experimental anharmonicities and mode frequencies.

Normal mode	assignment	Experimental frequency (cm^{-1})	Calculated diagonal anharmonicities (cm^{-1})						Experimental value (cm^{-1})
			Conf. I		**Conf. II**		**Conf. III**		
			6-31+ G(d,p)	6-311++ G(d,p)	6-31+ G(d,p)	6-311++ G(d,p)	6-31+ G(d,p)	6-311++ G(d,p)	
20	C-O as	1180	10.0	9.3	13.3	12.8	10.5	9.0	15
21	C-O ss	1250	-11.1	2.3	19.2	2.9	-2.7	9.0	13
22	CH_3 bending	1371	16.8	17.6	16.8	16.0	17.6	18.2	15
23	CH_2 scissoring	1371	-26.3	5.7	5.9	5.0	-9.3	6.2	-
24	CH_3 bending	1430	11.1	12.8	12.3	11.9	5.9	-2.1	-
25	CH_3 bending	1430	14.8	15.5	13.7	12.7	11.2	13.4	-
26	C=C stretch	1639	21.4	10.2	6.1	2.0	7.6	11.6	11
27	C=O stretch	1787	18.8	24.3	24.2	13.5	29.9	26.2	16
28	C≡N stretch	2236	23.0	22.8	24.2	22.9	23.1	22.6	22
29	CH_3 ss	2940	43.1	45.1	41.6	40.9	43.5	45.1	-
30	CH_3 as	2995	68.2	66.2	68.5	67.4	65.0	64.2	-
31	CH_2 ss	3046	90.8	89.3	90.8	89.4	89.5	119.5	-
32	CH_3 as	3046	88.2	86.7	79.8	73.8	106.6	87.7	-
33	CH_2 as	3135	64.8	65.2	78.5	74.7	66.1	66.8	44

Table S3. Computed diagonal anharmonicities for conformer I, II and III of the 1-cyanovinyl acetate with the normal modes frequencies higher than 1000cm^{-1} calculated at B3LYP 6-31+G(d,p) and 6-311++G(d,p) level in gas phase and experimental anharmonicities and mode frequencies.

Normal mode	assignment	Experimental frequency (cm^{-1})	Calculated diagonal anharmonicities (cm^{-1})						Experimental value (cm^{-1})
			Conf. I		**Conf. II**		**Conf. III**		
			6-31+ G(d,p)	6-311++ G(d,p)	6-31+ G(d,p)	6-311++ G(d,p)	6-31+ G(d,p)	6-311++ G(d,p)	
20	C-O as	1180	9.2	8.2	10.5	11.5	9.9	7.4	15
21	C-O ss	1250	12.4	-2.7	1.1	1.4	11.5	-1.1	13
22	CH_3 bending	1371	19.7	17.6	16.4	15.9	16.1	18.2	15
23	CH_2 scissoring	1371	-11.5	-7.4	5.7	12.9	-11.7	-4.6	-
24	CH_3 bending	1430	12.9	13.2	12.7	11.9	2.4	39.8	-
25	CH_3 bending	1430	15.8	15.8	12.3	12.5	15.2	6.4	-
26	C=C stretch	1639	11.2	1.5	3.0	3.9	2.9	10.0	11
27	C=O stretch	1787	18.3	13.9	22.2	22.3	27.1	22.5	16
28	C≡N stretch	2236	22.9	22.4	22.8	22.4	23.0	22.5	22
29	CH_3 ss	2940	43.2	43.3	41.0	40.8	42.3	95.4	-
30	CH_3 as	2995	67.6	65.5	62.9	61.9	65.6	63.8	-
31	CH_2 ss	3046	88.2	85.3	87.7	84.8	90.9	88.0	-
32	CH_3 as	3046	115.7	115.3	74.1	72.0	100.1	101.3	-
33	CH_2 as	3135	65.1	62.7	74.4	70.5	66.1	64.4	44

Table S4 Transition dipole moment cross angles from coupling red (bleaching) and blue (absorption) peaks measurements.

Pair number	Coupled modes	Relative angle (degree) Blue peak	Relative angle (degree) Red peak
1	C=C/C=O	64±3	78±5
2	C=C/C≡N	43±3	36±3
3	C=C/C-O(as)	37±5	37±5
4	C=C/CH_2(as)	37±5	38±3
5	C=C/CH_2(ss)	43±5	36±5
6	C=C/CH_3(as)	37±5	36±5
7	C=O/C≡N	58±3	69±5
8	C=O/C-O(as)	78±3	72±5
9	C=O/C-O(ss)	47±5	61±3
10	C=O/CH_2(as)	58±3	66±5
11	C=O/CH_3(as)	55±3	47±3
12	C≡N /C-O(as)	69±3	58±5
13	C≡N /CH_2(as)	47±5	55±5
14	C≡N /CH_2(ss)	37±5	42±3
15	C≡N /CH_3(as)	43±5	42±5
16	C-O(as)/CH_2(as)	55±3	54±3
17	C-O(as)/CH_2(ss)	51±3	61±5

The difference between two types of measurements for the same angle can be ~10 degree. There are three possible reasons. The first one, which we believe to be the most probable, is the intramolecular vibrational relaxation induced signal change. The typical lifetime of the modes is a few ps, and the best temporal resolution we can get is 200~300 fs. Therefore, it is sure that the vibrational decay will have some effects on the measurements. As we found before{Bian, 2009 #1619}{Bian, 2010 #1660}{Bian, 2010 #1694}, the influence of the relaxation on the read cross peak is much more severe than on the blue cross peak mainly because of the heat induced bleaching (this is the reason

why we always choose the blue peaks. The following comparison to the calculations seems to support our choice). The second one, which is in principle possible but less likely as the first one, is the combination excitation induced transition dipole moment change. This is related to the signal generation mechanism of the cross peaks. The red cross peak in the coupling case is the angle measurement between the 0-1 transitions of two coupled modes at the ground state. The blue cross peak is also the measurement between the 0-1 transitions of the two modes, but in this case the 0-1 transition of the second (excited) mode is excited while the first mode is at the first excited state (combination excitation). Therefore, if the excitation of one mode can severely change the other mode's transition, the red and blue cross peaks will give very different angles. To the best of our knowledge, we have not seen any systematic discussion and demonstration about this issue. To have a fair estimation about how big such an effect can be, we can use the frequency shift induced by the combination excitation (the probe frequency difference between the red and blue cross peaks). The typical frequency shift is only a few cm^{-1} as can be seen from our data, corresponding to less than 1% of the modes' vibrational frequencies. Intuitively, it would be difficult to image that such a small effect on the transition frequency of one mode can have a huge effect on the transition direction of the same mode. Nonetheless, rigorous theoretical studies and model systems are needed to clarify this point. The third reason, which is similar to the first one, is some possible fast nonresonant decay induced bleaching.

For the molecule studied here, the difference between the red and blue cross peaks is actually within the experimental uncertainty (~10 degree) induced by the fast molecular rotation (~4ps) because of its relatively small size. However, if we compare the

two measurements to the calculations (figure 5 (b) in the main text and fig. S5 in the following), the two measurements give the same molecular conformations but the experiment/calculation deviation of the red cross peak is about 2 degree bigger than the blue cross peak for the most probable molecular conformation.

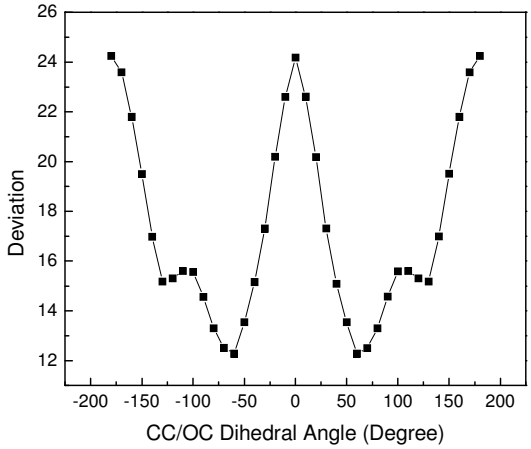

Figure S5. Deviation Er vs the CC/OC dihedral angle. The cross angles used for the calculation of Er are from the red peak data.